

Supplementary Information

A Gravity-driven Microfluidic Metering System for Automation of Multiplexed Bioassays

Lu Zhang ^{a 1}, Johnson Q. Cui ^{* b 1}, and Shuhuai Yao ^{* a,b}

^a The Department of Chemical and Biological Engineering, Hong Kong University of Science and Technology, Sai Kung, New Territories, Hong Kong.

^b The Department of Mechanical and Aerospace Engineering, Hong Kong University of Science and Technology, Sai Kung, New Territories, Hong Kong.

* Corresponding authors

E-mail address: qcui@connect.ust.hk, meshyao@ust.hk

¹ Lu Zhang and Johnson Q. Cui contributed equally to this work.

Content

Figure S1: The design and fabrication of the metering chip.

Figure S2: The metering performance with various input liquid volume.

Figure S3: Investigation of the minimum volume that can be dispensed by the metering system.

Figure S4: Investigation of the maximum number of cups that could be integrated into our metering system.

Figure S5: Characterization of opening time and activation temperature of the wax valves.

Figure S6: The measurement method for the dispensed volume in metering cups.

Figure S7: Workflow of the algorithm.

Figure S8: The standard curves of the fluorometric assays of glucose, uric acid, and total cholesterol.

Table S1: The detailed protocol for preparation of artificial urine samples.

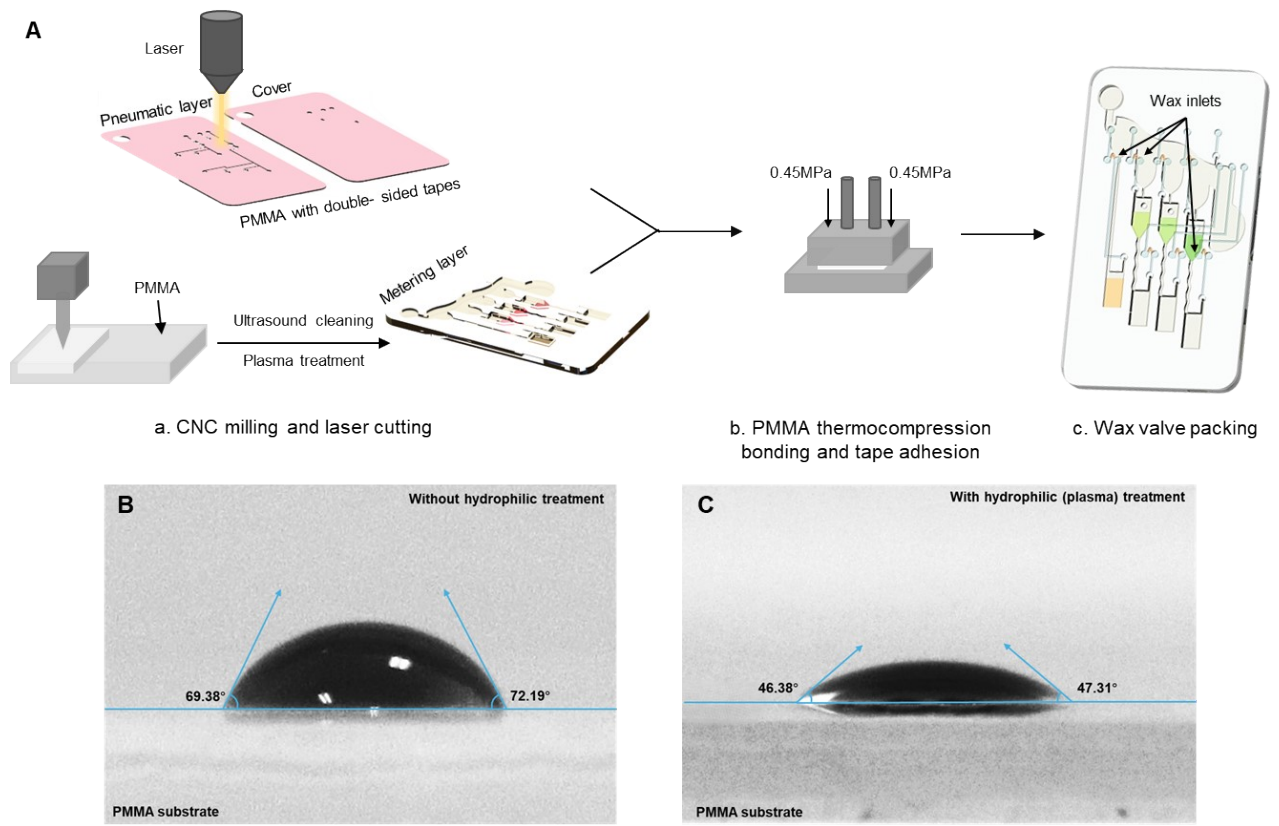


Fig. S1: The design and fabrication of the metering chip. (A) The fabrication process of the chip. The contact angle of 10 μL water droplet on the PMMA substrate without (B) and with (C) hydrophilic treatment.

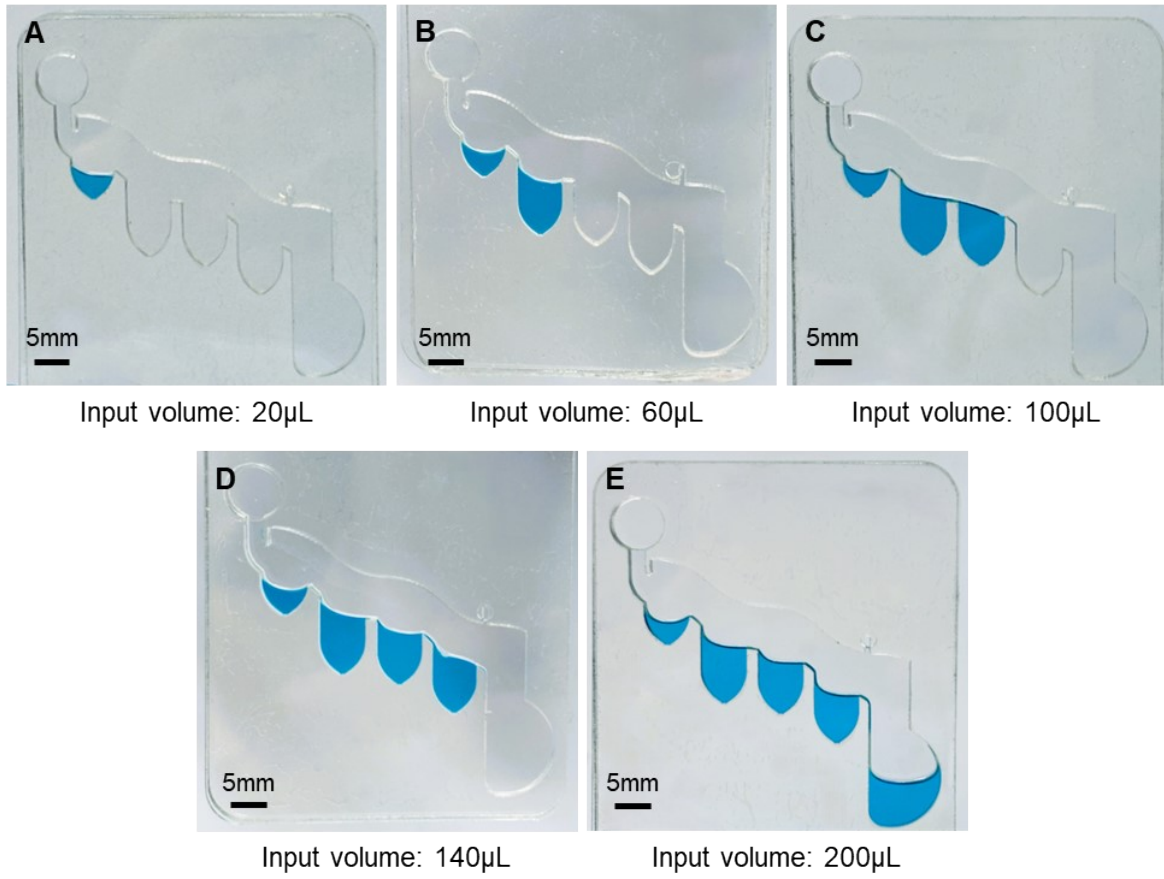


Fig. S2: The metering performance with various input liquid volumes.

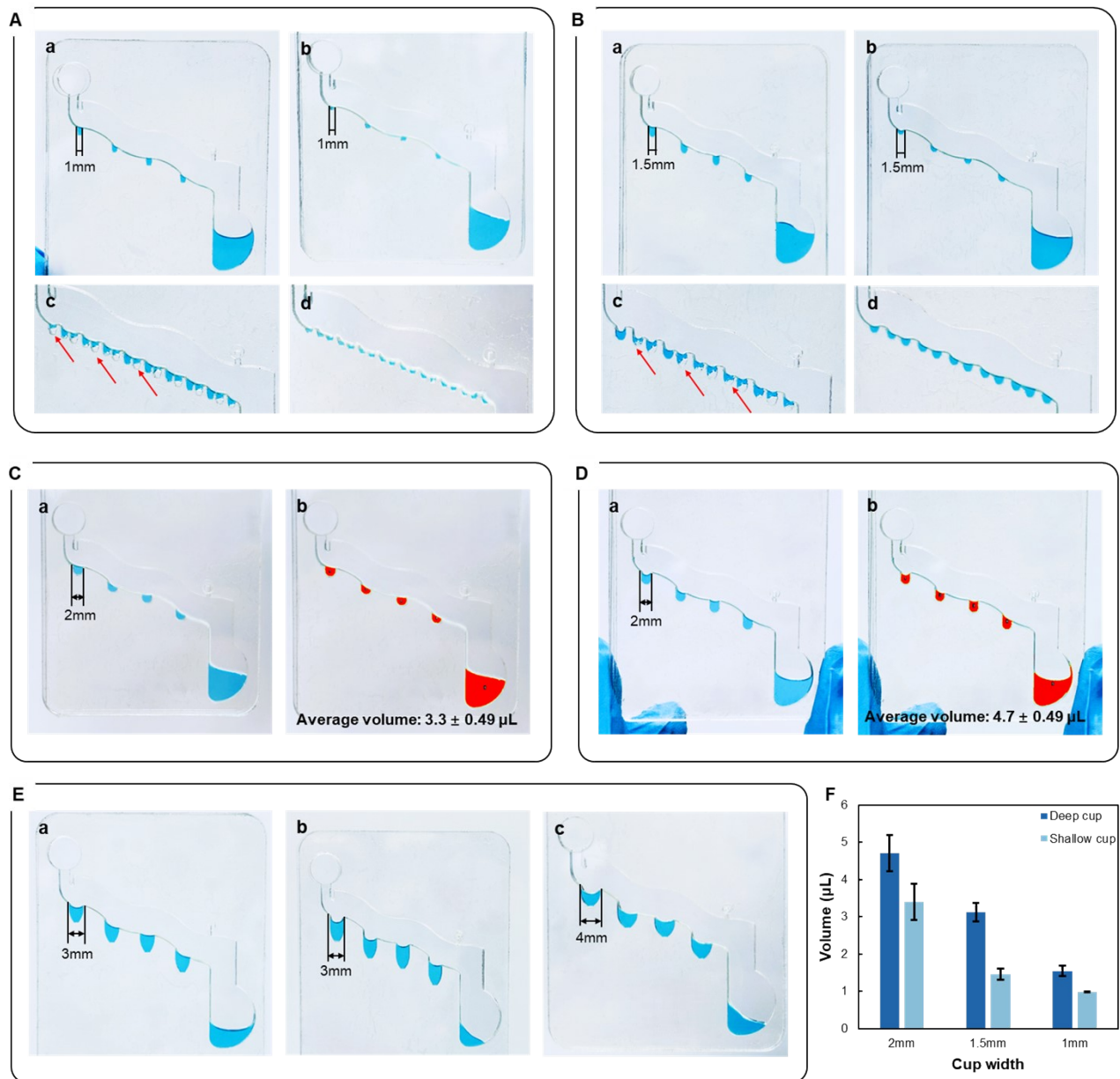


Fig. S3: Investigation of the minimum volume that can be dispensed by the metering system. (A) Metering results of cups with 1mm width. Cups with deep (a) and shallow (b) heights. Air bubbles trapped in the deep cups (c) and the potential siphon phenomenon in the shallow cups (d). (B) Metering results of cups with 1.5 mm width. Cups with deep (a) and shallow (b) heights. Air bubbles trapped in the deep cups (c) and the potential siphon phenomenon in the shallow cups (d). (C) Metering (a) and measurement (b) results of cups with 2mm width with shallow heights. (D) Metering (a) and measurement (b) results of 2 mm width cups with deep heights. (E) Metering results of 3 mm width cups with deep (a) and shallow (b) heights, and 4 mm width cups (c). (F) The dispensed volume of metering cups with different width. The minimum volume that can be consistently dispensed in our chip is $\sim 4 \mu\text{L}$.

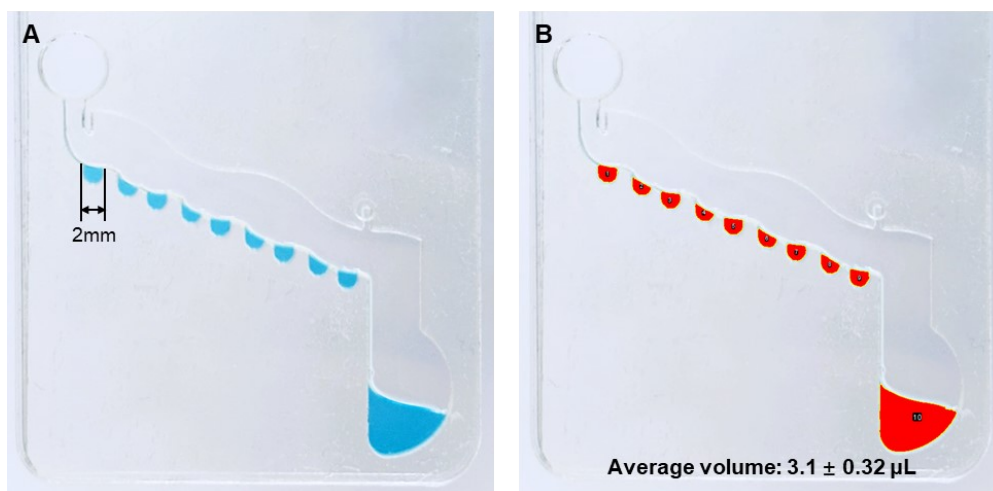


Fig. S4. Investigation of the maximum number of cups that could be integrated into our metering system. Metering results (A) and measurement results (B) of nine cups with a width of 2 mm.

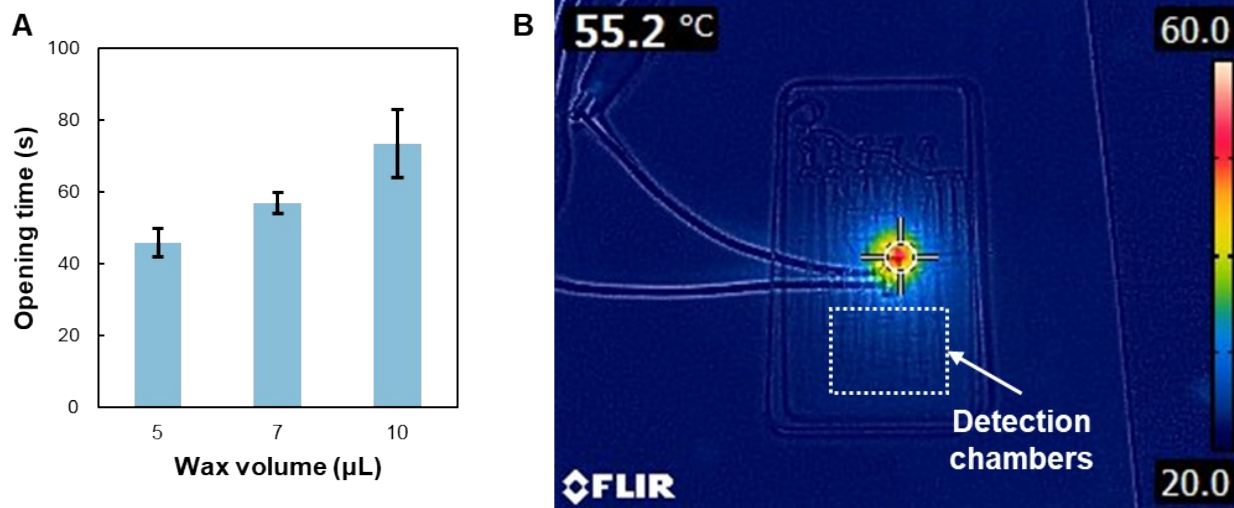


Fig. S5. Characterization of opening time and activation temperature of the wax valves. (A) Opening time of wax valves with different input volumes of wax. (B) Infrared image showing the temperature distribution while the heater is in operation.

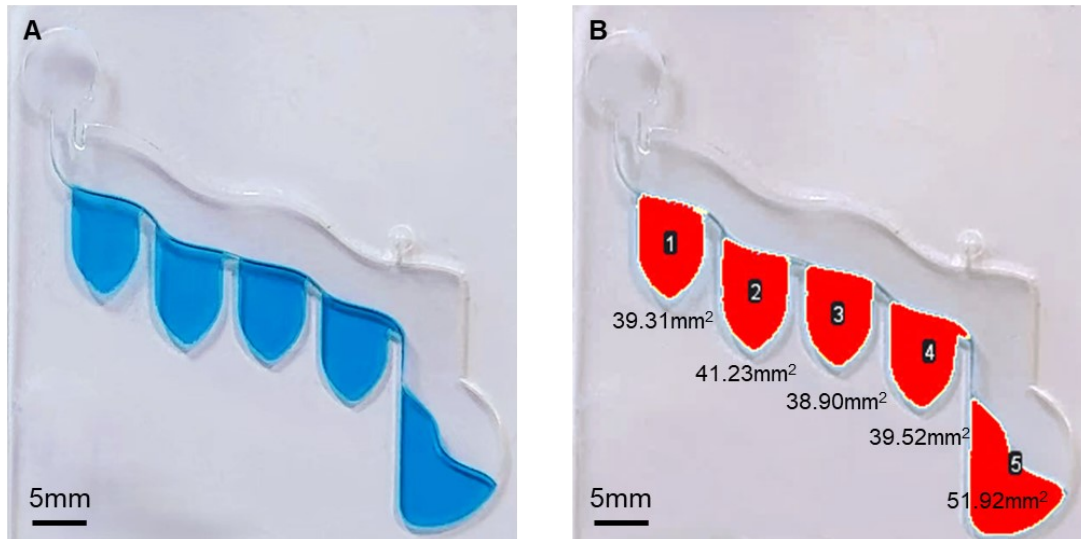


Fig. S6: The measurement method for the dispensed volume in metering cups. The images were analyzed using ImageJ, where the areas with the liquid are segmented and measured, the final volume is calculated by the multiplication of the surface area with chamber depth (~1 mm).

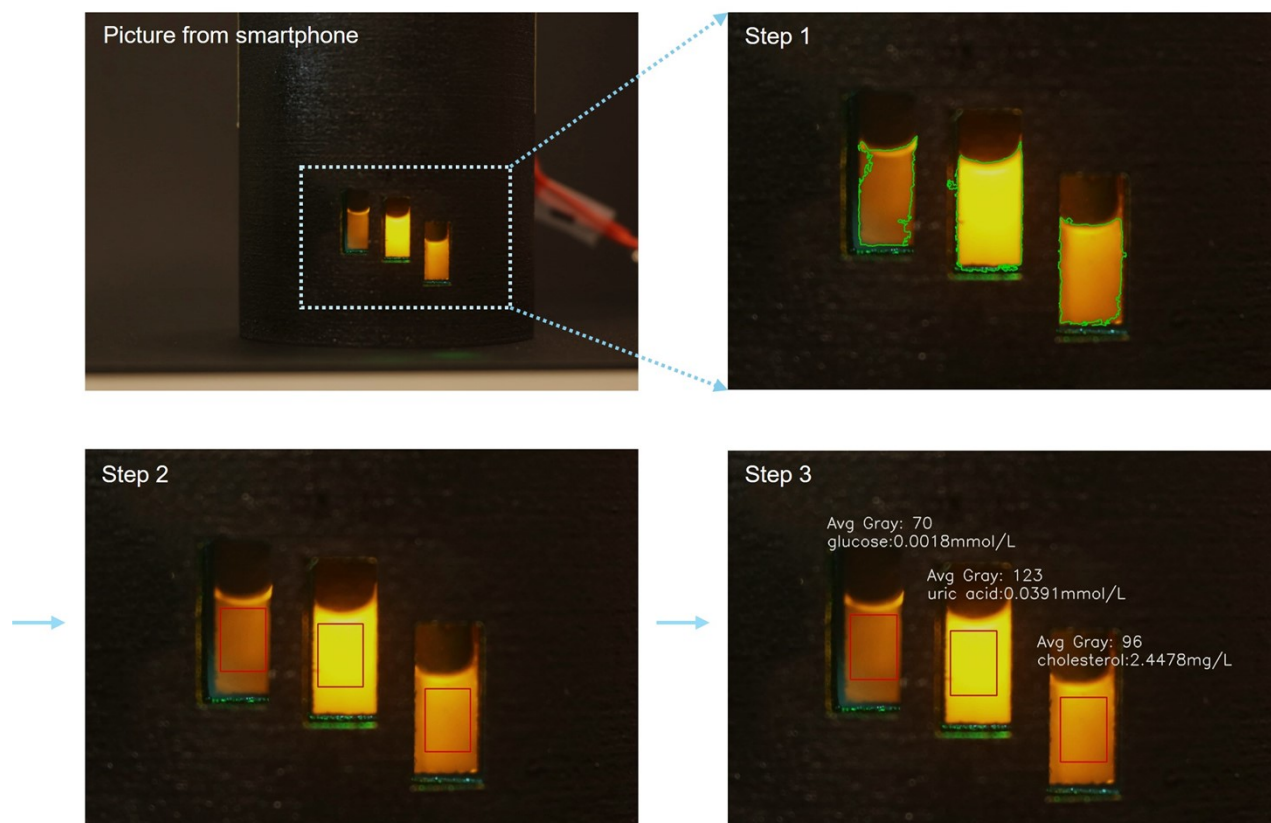


Fig. S7: Workflow of the algorithm. Step 1: recognition of fluorescence area; Step 2: determination of region of interest (ROI), in this step, the center point for the fluorescence area is determined by averaging the x coordinates and the y coordinates. Next, a rectangle is overlaid on top of the fluorescence area with the same center point. The size of the rectangle is set so that it entirely sits within the fluorescence area while covering sufficient area for measurement, which eliminates the signal fluctuation at the liquid boundaries; Step 3: calculation and display of gray value and final concentration.

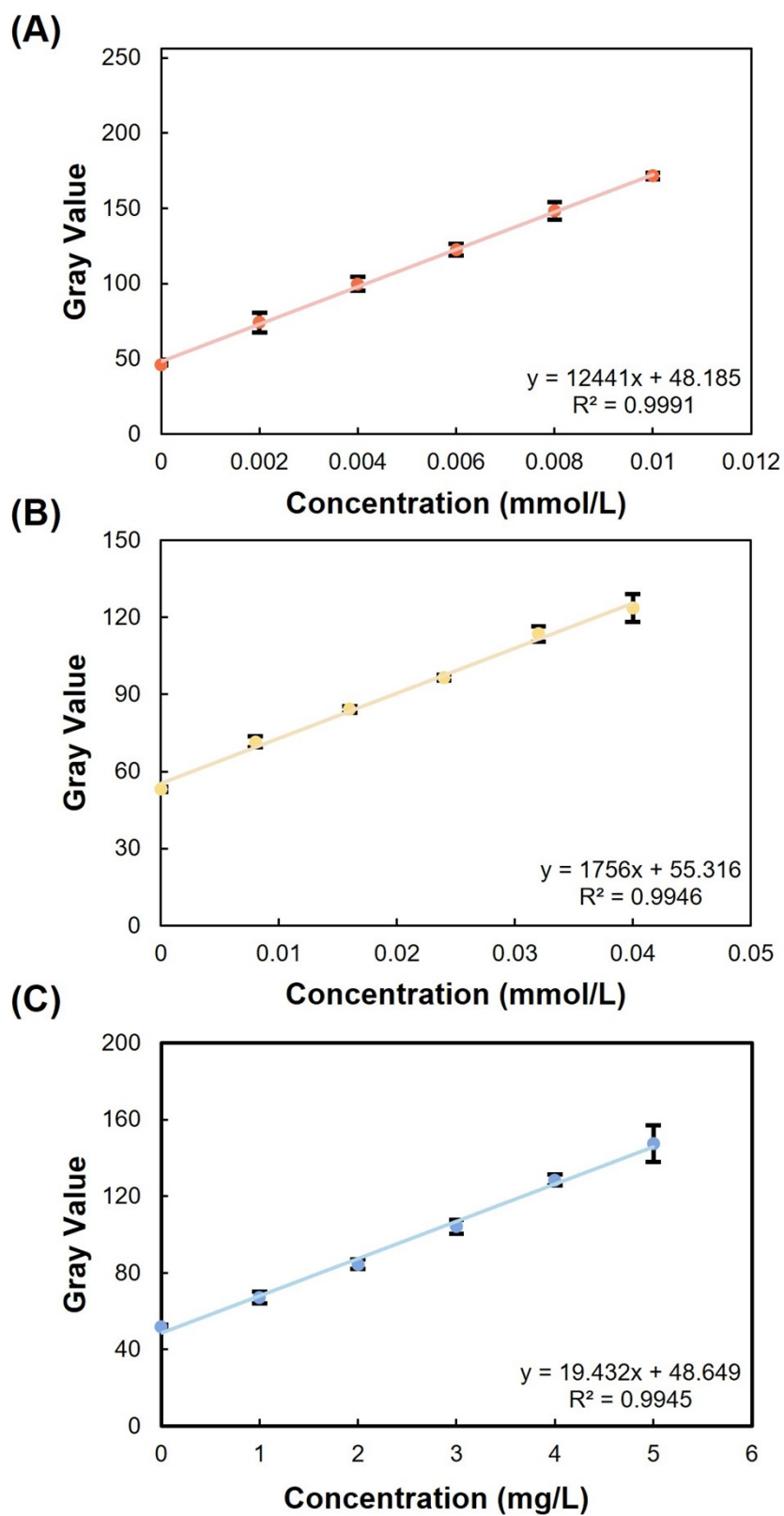


Fig. S8: The standard curves of the fluorometric assays of glucose (A), uric acid (B), and total cholesterol (C).

Table S1: The detailed protocol for spike addition to artificial urine samples.

Group No.	Spiked targets						Artificial urine Volume (µL)	Eventual concentration (theoretical)		
	Glucose (mmol/L)		Uric acid (mmol/L)		Total cholesterol (mg/L)			Glucose (mmol/L)	Uric acid (mmol/L)	Total cholesterol (mg/L)
	Concentration (mmol/L)	Volume (µL)	Concentration (mmol/L)	Volume (µL)	Concentration (mg/L)	Volume (µL)				
Control	0	0	0	0	0	0	140.00	0.0000	0.0000	0.0000
1	0.10	35.00	0	0	0	0	105.00	0.0040	0.0000	0.0000
2	0	0	0.20	70.00	0	0	70.00	0.0000	0.0160	0.0000
3	0	0	0	0	25.00	70.00	70.00	0.0000	0.0000	2.0000
4	0.10	30.00	0.04	37.50	0	0	82.50	0.0080	0.0040	0.0000
5	0.01	37.50	0	0	37.50	5.00	75.00	0.0010	0.0000	0.5000
6	0	0	0.20	60.00	25.00	60.00	30.00	0.0000	0.0320	4.0000
7	0.10	18.75	0.20	37.50	25.00	445.00	48.75	0.0050	0.0200	3.0000
8	0.01	30.00	0.04	18.75	5.00	37.50	63.75	0.0008	0.0020	0.5000